Mechanism Study of Porcine Skin Ablation by Nanosecond Laser Pulses at 1064, 532, 266, and 213 nm

Xin-Hua Hu, Qiyin Fang, Mickael J. Cariveau, Xiaoning Pan, and Gerhard W. Kalmus

Abstract—The ablation mechanism of fresh porcine skin has been studied using nanosecond laser pulses at the wavelengths of 1064, 532, 266, and 213 nm. We have identified the Na spectral line at 589 nm in the secondary radiation from the ablated skin sample as the signature of tissue ablation and measured the ablation probability near ablation threshold. Ablation depth per pulse has been measured by histological examination of ablated skin samples. Review of the ablation probability data through probit analysis indicated that the same mechanism is likely to be operative for tissue ablation at all four wavelengths. Various soft tissue ablation models are discussed, and it is concluded that the ablation of the skin by nanosecond laser pulses from 1064 to 213 nm is a result of electronic impact ionization which leads to the formation of a plasma.

Index Terms—Avalanche breakdown, biomedical applications of optical radiation, biological tissues, laser ablation, neodymium:YAG lasers, spectral analysis.

I. INTRODUCTION

IN THE progression of less-damaging surgical laser procedures and smaller laser systems, nanosecond laser pulses have gained wide acceptance because these pulses can be generated with large pulse energies from compact solid-state laser systems such as Q-switched systems. Although nanosecond laser pulses have been used widely for two decades, ranging from refractive keratotomy to treatment of pigmented lesions, comprehensive studies of the fundamental mechanisms underlying the tissue ablation are relatively recent. Early investigations of tissue ablation by short laser pulses have led to three major models: the selective photothermolysis model and its variations [1]–[3], the photochemical model [4], [5] and the plasma-mediated ablation model [6]–[9]. The selective photothermolysis model presumes a photothermal mechanism, or heating by light absorption through radiationless relaxation, that considers the thermally induced mechanical pressure as the cause of tissue ablation. The photochemical model, on the other hand, conjectures that the pressure increase is a result of photochemical dissociation of the macromolecular bonds due to the large photon energy of the deep ultraviolet light.

Both models consider the absorption of laser light energy by the tissue necessary to initiate the ablation and take into account the various thermal and mechanical effects. In contrast, plasma formation or optical breakdown in tissue caused by the strong electromagnetic field of the short laser pulses has been assumed in the plasma-mediated ablation model to induce tissue ablation. Light absorption can be accomplished by the induced plasma and ablation of nonabsorbing tissue becomes possible.

The plasma model has been widely accepted for tissue ablation by picosecond and femtosecond laser pulses because of the very high peak irradiance resulting from the ultrashort pulses. The occurrence of plasma in the tissue ablated by nanosecond pulses has been established in ocular tissues in the visible and near-infrared regions because the tissues are nearly transparent and tissue ablation with a visible flash or bubble can be observed [6]–[9]. Ablation of corneal tissue with ultraviolet picosecond pulses at 263 and 211 nm has also been explained by the plasma model for the dependence of the ablation depth on laser fluence [10]. However, for soft biological tissue ablation by nanosecond pulses, the characteristics of the plasma-mediated ablation model need to be further elucidated, and acceptance of the plasma model is far from ubiquitous [11], especially when tissue absorption becomes significant as the light wavelength approaches the ultraviolet region. It appears that the ambiguity of the fundamental mechanism underlying tissue ablation by nanosecond laser pulses is, to a large extent, related to the lack of quantitative studies of the ablation process near the threshold. Given this fact, we have studied the ablation of fresh porcine skin *in vitro* using nanosecond laser pulses at 1064, 532, 266, and 213 nm. Besides the inherent importance of studying fundamental mechanisms, a clear understanding of the ablation process of soft tissue by nanosecond laser pulses will benefit the exploration of new approaches in the surgical applications of Q-switched lasers [12]. In this paper, we present the spectral analysis of secondary radiation and histological analysis of ablated porcine skin samples near ablation threshold. Based on these results, we established the spectral line at 589 nm from the excited Na atoms as the signature of the tissue ablation process and have measured the ablation probability at the four ablating wavelengths. The ablation mechanism is investigated through probit analysis of the ablation probability data and discussed in light of the plasma-mediated ablation model.

TABLE I
FOCAL SPOT DIAMETERS AND ABLATION THRESHOLDS

Ablation Wavelength λ (nm)	1064nm	532nm	266nm	213nm
$2w_{0x}$ (μm)	14	25	20	20
$2w_{0y}$ (μm)	18	25	20	20
$\dfrac{dY}{d\log I}$ {1}	5.23	9.26	6.02	7.08
F_{th} (J/cm^2) @ P =90% {1}	129	35.8	14.3	1.6
W_{th} @ P=90% {1}	0.256mJ	0.176mJ	44.9μJ	5.14μJ
E_{th} (V/m) @ P =90% {1}	1.68×10^8	7.72×10^7	5.38×10^7	1.96×10^7
F_{th} (J/cm^2) @ P =10% {1}	41.8	18.9	5.36	0.711
K (V/m)	1.06×10^9	6.58×10^8	3.88×10^8	1.43×10^8
α (cm^{-1}) {2}	5	1	$\sim$ 600	N/A

{1} obtained from the regression lines in Fig. 3(a).
{2} absorption coefficients of skin epidermis are from [21]
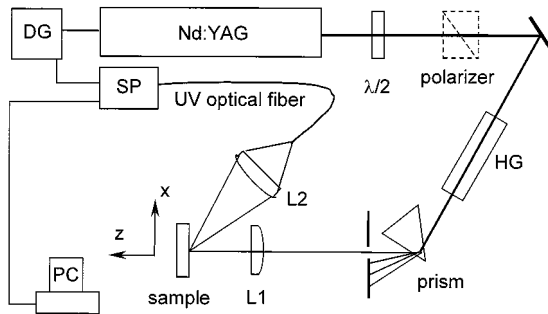

Fig. 1. Schematics of the experimental setup. DG: digital delay generator. HG: harmonic generator assembly. L1: the focusing lens. L2: the secondary radiation collection lens. SP: CCD spectrometer. PC: personal computer for stepping motor control and data acquisition from the spectrometer.

II. MATERIALS AND METHOD

A Q-switched Nd:YAG laser (Surelite I, Continuum) was used to generate pulses of 100 mJ energy and 14-ns duration at the fundamental wavelength of 1064 nm. The pulse energy was adjusted by a half-wave plate and a polarization cube. The pulse-to-pulse energy fluctuation was determined to be ±5%. For experiments requiring pulse energies less than 5 mJ at 1064 nm, an optical wedge and mirrors were inserted before the half-wave plate to use only the portion of the beam reflected from the front surface of the wedge for reducing the excessive distortion of the beam profile after the polarization cube. A plano-convex lens of 75-mm focal length was employed to focus the laser beam of 0.6 mrad divergence onto the skin sample surface. Based on an f-number of $f/10.7$ the spherical aberrations of the focusing lens were estimated to be negligible in comparison to the focal

spot diameter [13]. The beam quality was examined using a CCD beam profiling system (PC 300, Spiricon) with a lens of 75-mm focal length. M_x^2 and M_y^2 [14] in the transverse plane of the beam were determined to be 1.31 and 1.29, respectively. Using the M^2 method, we determined the beam diameters at the focal spot, defined at the e^{-2} point relative to the peak irradiance, to be $2w_{0x} = 14 \pm 1$ μm and $2w_{0y} = 18 \pm 1$ μm at 1064 nm, which was verified by the knife-edge method [15].

To acquire nanosecond pulses at 532, 266, and 213 nm, we replaced the polarization cube with a harmonic generator unit. The unit contains an inverted telescope to produce a collimated beam with a reduced diameter of 5 mm at 1064 nm before entering three type I BBO crystals of $7 \times 7 \times 7$ mm^3 size. The first BBO crystal was used to generate second harmonic pulses at 532 nm, which can be reflected out of the unit by three harmonic separating mirrors to reduce the 1064-nm component in the output beam to less than 0.2% of its initial pulse energy. The 266- and 213-nm pulses were obtained with additional BBO crystals and separated from the 1064- and 532-nm pulses using an ultraviolet prism. The measurement of the harmonic beam profiles using a 75-mm focal length lens with the CCD beam profiling system confirmed that the transverse profiles were nearly Gaussian and symmetric in the x- and y-axes. The diameter of the beam at the focal spot after the focusing lens was determined by the knife-edge method and is listed in Table I for different laser wavelengths. The schematic of the experimental setup is shown in Fig. 1.

Fresh skin patches were obtained from the dorsal neck area of white domestic six-month old pigs from the Brody School of Medicine at East Carolina University or adult pigs from a local abattoir. The skin patches were stored within crushed ice
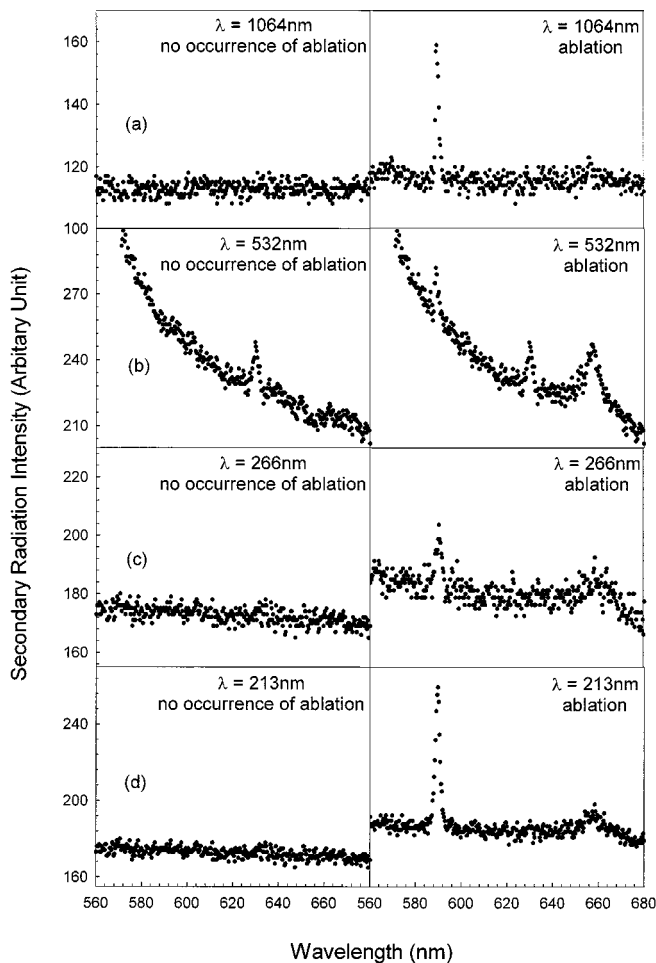
Fig. 2. Typical secondary radiation spectra from ablated tissue samples measured by the CCD spectrometer at different ablating wavelength λ. Each pair of diagrams were obtained at the same laser fluence near the 90% ablation probability.

(∼4 °C) immediately after removal from the pig. The sample sizes of about 2×5 cm^2 were prepared by removing the hair and subcutaneous tissue and warmed to room temperature (∼25 °C) with 0.9% saline drops. The skin sample was clamped onto a holder with the epidermis facing the laser beam with translation in the horizontal direction by a stepping motor to ensure that each laser pulse was delivered on a fresh spot for experiments under a single-pulse condition. Before each experiment, the sample holder was carefully aligned along the laser beam axis with a precision translator so that the sample surface was at the beam waist. All measurements were performed at room temperature within 30 h of animal euthanasia. Furthermore, the skin sample surface was moistened with saline solution every 5 min to keep it from dehydrating during the experiment. A separate study of porcine skin samples showed that the absorption coefficient at 1064 nm exhibits no change in the skin samples up to 30-h postmortem under identical storage conditions [16]. To quantitatively study the ablation process near threshold, we measured the spectrum of secondary radiation from the ablated skin sample surface under the single-pulse condition by translating the sample during the ablation and lowering the pulse repetition rate to 0.2 Hz to allow for spectrum acquisition. The secondary radiation was collected by a spherical lens of 100-mm

focal length and 38-mm diameter into an optical fiber of 600-μm diameter which is connected to a spectrometer of 5-nm resolution with a linear CCD array detector[1] .

To verify tissue ablation, we measured the ablation depth per pulse at each of the four ablating wavelengths under a multiple-pulse condition. On each sample, a series of six or seven lines was ablated at different pulse energies with a 1-mm separation between the lines. For ablation depth measurements, the pulse repetition rate was increased to 10 Hz. The speed of the translator was adjusted according to the spot size so that the pulse number per spot was kept at either 45 or 90 in order to increase the sensitivity of the ablation depth measurement and to avoid cutting through the full-thickness of the skin sample. Ablated samples were immediately fixed in Bouin's fixative for 12-h after ablation. Tissue cross sections were obtained by routine histological procedures with each ablation depth measured under a microscope as an average from 40–60 sections. One ablation curve was obtained for each sample at ablating wavelengths in which the ablation depth per pulse is plotted as a function of laser fluence.

III. RESULTS

To quantitatively study the tissue ablation process near threshold on an objective basis, we chose to identify the ablation through optical measurement of the secondary radiation that have been used for labeling optical breakdown in aqueous solutions [17]. The secondary radiation spectra were analyzed between 300 and 800 nm at each of the four ablating wavelengths near the ablation threshold using the CCD spectrometer. Two spectral lines at 589 and 656 nm within the spectral window were initially identified as the signature of tissue ablation with 1064-nm pulses because they are coincident with the weakest sparks visible to dark-room adapted eyes. Using a Czerny-Turner monochromator of 0.05-nm resolution (270 MX, McPherson), the peak positions of the two lines were determined to be 589.04±0.08 and 656.32±0.5 nm, which can be associated with electronic transitions in the neutral Na and H atoms, respectively [18]. Among the two spectral lines obtained near threshold, the narrow Na spectral line was clearly distinguishable from the background when the tissue sample was ablated with 1064-nm pulses and from the scattered and fluorescence light with 532-, 266-, and 213-nm pulses, while the H$_\alpha$ line was weak and broad. Typical spectra for identification of tissue ablation at ablating wavelengths of 1064, 532, 266, and 213 nm are shown in Fig. 2. To determine the origin of the Na line at 589 nm, we repeated secondary radiation measurements with skin tissue samples moistened only with distilled water. Although the Na line became weaker as expected, the spectral line was observed clearly above the background with the same relation between the probability of line appearance and laser fluence near ablation threshold as the one measured from saline treated samples. On the other hand, we observed that the spectral line at 656 nm is a result of optical breakdown in air since this line can be eliminated by immersing the tissue sample in distilled water. Combining these results, we determined to use the spectral line at 589 nm
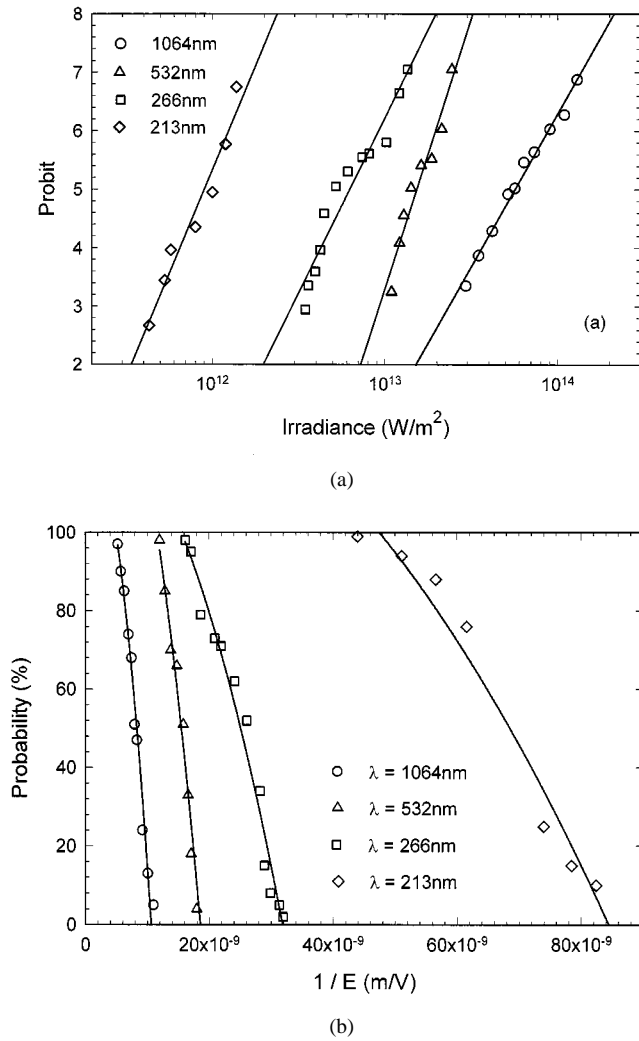
[1]S2000, Ocean Optics

(a)

(b)

Fig. 3. (a) Probit Y of the ablation probability as a function of irradiance I at different ablation wavelength. Each probability data point was obtained with 100 pulses at the same laser fluence. Straight lines are regression lines for each set of data following an equation $Y = \alpha + \beta \log(I)$, where α and β are fitting parameters. (b) The same data plotted with ablation probability P as a function of the inverse of the rms electric field E of the laser pulses. Solid lines are fitting curves for each set of data following an equation $P = P_0 \exp(-K^2/E^2)$, where P_0 and K are fitting parameters.

as the signature of the tissue ablation and found that the tissue ablation process near threshold is of probabilistic nature at all four ablating wavelengths.

The ablation probability near threshold was obtained by the ratio of the appearance of the secondary radiation line at 589 nm to the laser pulses delivered to the sample under a single-pulse condition. In each measurement, 100 pulses were used to measure the ablation probability P as a function of the laser fluence F at 1064, 532, 266, and 213 nm by varying the pulse energy. To investigate the ablation mechanism operative at the four wavelengths, the ablation probability data have been studied using probit analysis. Fig. 3(a) shows a plot of the probit of percentage probability P against the logarithm of the irradiance I. The probit Y is related to P as [19]

$$P = \frac{1}{\sqrt{2\pi}} \int_{-\infty}^{Y} \exp\left\{\frac{1}{2}u^2\right\} du \qquad (1)$$
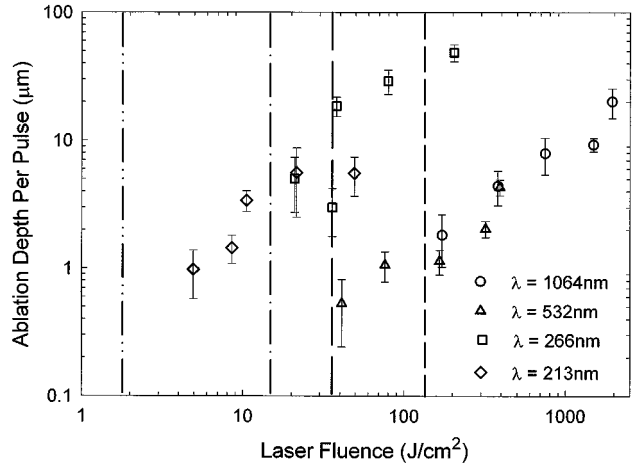

Fig. 4. Ablation depth per pulse versus laser fluence at different ablation wavelength λ. The number of pulses per spot $N = 90$ were used for $\lambda = 1064$ and 532 nm and $N = 45$ for $\lambda = 266$ and 213 nm. The error bars indicate the fluctuation in the depth measurement from multiple tissue sections and the vertical lines mark the position of laser fluence threshold $F_{\mathrm{th}} @ P = 90\%$ obtained from Fig. 3(a), with short dashed line for $\lambda = 1064$ nm, a long dashed line for $\lambda = 532$ nm, a dashed-dotted line for $\lambda = 266$ nm, and a dashed-dotted-dotedt line for $\lambda = 213$ nm.

and the irradiance I of the laser pulse is determined from the following equation:

$$I = \frac{F}{\tau} = \frac{W}{\pi w_x w_y \tau} \qquad (2)$$

where W is the pulse energy and τ is the pulse duration. From Fig. 3(a), it is clear that the percentage probability follows a normal distribution with respect to $\log(I)$. The experimental data at each of the four ablating wavelengths were fitted to a straight regression line to determine the slope $(dY)/d(\log I)$ and ablation thresholds in pulse energy W_{th}, laser fluence F_{th}, and electric field strength E_{th} at probabilities of 10% and 90% (see Table I). The average rms electric field strength E is calculated by $E = \sqrt{F/(\tau c n \varepsilon_0)}$, where c is the speed of light, and ε_0 is the permittivity in vacuum while the refractive index of the hydrated skin n is assumed to be 1.33. To further analyze the ablation mechanism, we also plotted the ablation probability P in Fig. 3(b) as a function of $1/E$. The dependence of the probability P on the electric field E was fitted to the equation $P = P_0 \exp(-K^2/E^2)$, where P_0 and K are fitting parameters.

The concurrence of the secondary radiation spectral line at 589 nm with tissue ablation was verified at laser fluences near the 90% ablation threshold by the measurement of ablation depth in the porcine skin. The skin sample was translated along the x axis for ablation under the multiple-pulse condition at a pulse repetition rate of 10 Hz. The translation speed was set to obtain the laser pulse number per spot, N, as 90 for ablation at 1064 and 532 nm and as 45 for 266 and 213 nm so that the ablation depth at the ultraviolet wavelengths would not exceed the full thickness of the skin at maximum laser fluence. The average and standard deviation of the ablation depth data were determined from histological sections prepared from the ablated tissue samples at each wavelength. The results are plotted in Fig. 4.

IV. DISCUSSION

We analyzed the secondary radiation spectroscopically from fresh porcine skin samples to establish the spectral line at 589 nm radiated from the ablated tissue as the signature of tissue ablation at 1064, 532, 266, and 213 nm. The narrow line at 589 nm from the Na atoms in the tissue distinguishes itself clearly from background and/or fluorescence light and can be enhanced by treating the tissue with 0.9% saline solution. By identifying the signature spectral line, we were able to determine unequivocally the probabilistic nature of the skin tissue ablation process and quantitatively measure the ablation probability with nanosecond laser pulses at the four wavelengths. To facilitate the comparison between the two types of experimental results, the laser fluence thresholds at $P = 90\%$ determined from the probability measurements are marked by dash and dashed-dotted lines in Fig. 4. While the probability and ablation depth measured histologically were conducted under different conditions, single-pulse versus multi-pulse in different skin samples, we observed that tissue ablation occurs near the laser fluence thresholds measured at 90% probability from the secondary radiation. This directly confirms that the secondary radiation is a result of tissue ablation for all four wavelengths.

A large body of knowledge has been obtained on tissue ablation by nanosecond laser pulses over the last two decades [1]–[9]. It has become clear that the photochemical model is of limited significance to explain the experimental data for ablation with ultraviolet pulses. Variations from the selective photothermolysis model have been proposed to understand the mechanism of soft tissue ablation by nanosecond pulses in the spectral region from ultraviolet to near-infrared [2], [3]. It was suggested that overheating occurs at various chromophores in tissues through radiationless relaxation of the absorbed light energy, or thermalization, which induces explosive boiling of the water content in tissues and significantly lowers the threshold energy of ablation calculated for homogeneous absorption. A thermoelastic model further takes into account the inertial confinement as a result of rapid heating [2], [3]. However, the assumption of thermalization as the cause of tissue ablation underpins the above models and fails to explain our results presented in this paper on the probabilistic nature of the ablation at all four wavelengths at which the skin tissue exhibits large variations in light absorption. A plasma-mediated ablation model has been used to understand the ocular tissue ablation and water breakdown by visible and near-infrared nanosecond laser pulses to which the tissues or water have little absorption [6]–[9]. From the probit analysis of ablation probability shown in Fig. 3(a), one can see clearly that the tissue ablation processes near threshold at the four wavelengths are characterized by similar normal distributions in their ablation probability frequency. The slope of the regression lines fitted to the probit data at the ultraviolet wavelengths of 266 and 213 nm are between that of 1064 and 532 nm, as shown in Table I. Thus, it is indicated that the operative mechanism in the skin tissue ablation by nanosecond laser pulses at 266 and 213 nm is likely to be the same as that at 532 and 1064 nm [20]. This characteristic of ablation processes observed at different laser wavelengths is remarkable, considering that the linear absorption coefficient of the skin at the ablating

wavelength of 1064 nm is several orders of magnitude smaller than that at 266 nm [21] (absorption coefficient for 213 nm is unavailable).

The probabilistic nature of the skin ablation process near the threshold by the nanosecond laser pulses at 1064, 532, 266, and 213 nm is very typical of optical breakdown in condensed matter caused by short laser pulses [22]. The breakdown process can be analyzed through a rate equation describing the time dependence of the free electron density $\rho(t)$ under the influence of the optical radiation field [9], [22]

$$\frac{\partial \rho(t)}{\partial t} = (\eta - g)\rho(t) + \left(\frac{\partial \rho(t)}{\partial t}\right)_m \qquad (3)$$

where η is the cascade ionization rate given by the probability per unit time that a free electron has an ionizing collision with a bound electron, g is the rate of electron loss due to recombination, trapping, and diffusion out of the focal volume of the beam, and the last term on the right-hand side represents multiphoton ionization. Using the parameters that are relevant to the skin and the laser fluence threshold obtained from Table I, we determined that the cascade ionization rate $\eta\rho(t)$ is much greater than the multiphoton ionization rate $(\partial \rho(t)/\partial t)_m$ by nearly five orders of magnitude, at the ablation threshold for the 14-ns pulses at 1064 nm because of the low irradiance required at the threshold of skin ablation. A similar conclusion was drawn by skin ablation at 532 nm. Therefore, we concluded that the tissue ablation processes at these two wavelengths may be explained by the plasma-mediated model in which the plasma is induced through cascade ionization or impact ionization. For tissue ablation at 266 and 213 nm, however, the absorption of laser radiation by the skin tissue becomes large and the ablation thresholds decrease significantly as shown in Table I. From preliminary measurement of the absorbance of two porcine dermis samples of thicknesses between 50 and 100 μm, obtained with a cryostat microtome [23], we found that the attenuation coefficient doubles as the wavelength decreases from 260 to 220 nm in comparison to a modest increase of about 40% from 400 to 260 nm. These results indicate that the strong tissue absorption affects only the ablation threshold without modifying the nature of the probabilistic process near threshold. The existing plasma-mediated ablation model [22] is based on the assumption of negligible absorption and is not directly useful to understand the dependence of ablation threshold on tissue absorption.

To analyze the cascade ionization process, two microscopic mechanisms have been proposed for electrons to absorb energy from the optical radiation field [17], [22], [24]. The first mechanism postulates that some electrons avoid momentum-relaxing collisions and accelerate under the influence of the laser field, leading to an ionization probability given by $P = P'_0 \exp(-K'/E)$. The second mechanism, however, assumes that electrons may suffer momentum-relaxing collisions during acceleration but maintain their energies through the collisions. The corresponding probability can be shown to be given by $P = P_0 \exp(-K^2/E^2)$ [23]. The logarithm of the breakdown probability measured at the four ablating wavelengths, shown in Fig. 3(b), all have displayed a parabolic dependence on $1/E$ and thus are fitted to $P = P_0 \exp(-K^2/E^2)$. The similarity of the ablation probability dependence on the electric field of the
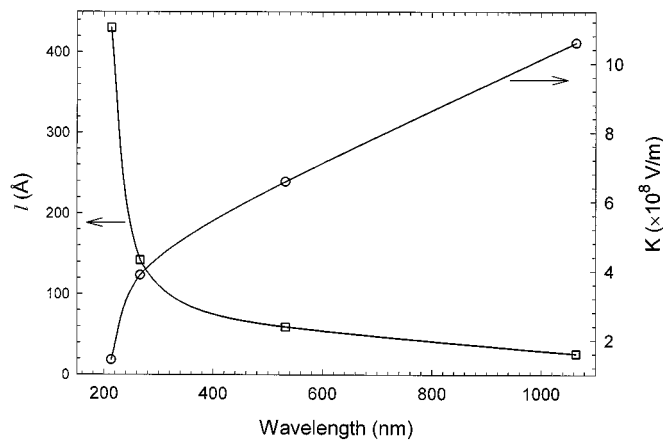
Fig. 5. Dependence of the K parameter of (1) and the electron mean free length defined in (4) on the wavelength of the nanosecond laser pulses. The solid lines are for guide of the eye.

laser pulse suggests that impact ionization causes the tissue ablation in the wide spectral range from near-infrared to ultraviolet and the seed electrons suffer elastic collisions before being freed and energized to start the cascade or impact ionization. The ablation thresholds in the rms electric field of the nanosecond laser pulses determined from our experiments range between 2×10^8 and 2×10^7 V/m, demonstrating the large electromagnetic fields generated at the ablation thresholds. The fitting parameter K can be derived as a function of photon energy $\varepsilon = h\nu$ [17], [24] and a mean free path of the accelerated electrons l, from which l is found as

$$l = \frac{\sqrt{\varepsilon_i \varepsilon}}{eK} \tag{4}$$

where ε_i is the ionization energy of the medium and e is the charge of the electron. Although (4) was obtained for electron ionization in crystals without significant light absorption, we may use it to estimate some mean free path of the seed electrons undergoing drift and momentum-relaxing collisions before being ionized in the skin sample. The dependence of the K parameter, listed in Table I, and the mean free path l, defined in (4), on the ablating wavelength are plotted in Fig. 5 assuming the ionization energy ε_i =6.5 eV for water in the skin. With the postulation that the ionization energy remains nearly constant for all the ablating wavelengths, we hypothesize that the steep increase in l between 266 and 213 nm be attributed to a similar steep increase in skin tissue absorption. It is plausible that the strong tissue absorption at the ablating wavelength of 213 nm can ionize a large number of seed electrons with low starting energy because of the high energy of the incident photons. If we further assume that electron–electron scattering dominates the initial process of ionization, the mean free path of the seed electrons should increase because of low starting energy resulting from statistical fluctuations [25]. Further investigations on the ultraviolet optical properties of porcine skin and theoretical modeling of ablation are currently in progress.

In summary, we have identified the spectral line at 589 nm from Na atoms as the signature of tissue ablation by nanosecond laser pulses at 1064, 532, 266, and 213 nm. With this optical signature, we were able to determine the probabilistic nature of the ablation process near the thresholds and measure the ablation probability as a function of laser fluence for the four ablating wavelengths. The ablation thresholds were obtained from the probability measurements and the possible mechanism underlying skin tissue ablation were analyzed. Based on these results, we concluded that the existing model of plasma-mediated ablation needs to be modified by taking tissue absorption into account to understand soft tissue ablation by nanosecond laser pulses in a wide optical spectrum from near-infrared to ultraviolet. A final point worth mentioning is that the dependence of the ablation threshold in laser fluence on the tissue absorption coefficient is fairly weak under the conditions of a small focal spot and nanosecond pulse duration. This suggests the possibility that the ablation of pigments and/or chromorphores with a large variation in optical absorption is possible using nanosecond laser pulses at a single wavelength in a tightly focused beam [12].

REFERENCES

[1] R. R. Anderson and J. A. Parrish, "Selective photothermolysis: Precise microsurgery by selective absorption of pulsed radiation," *Science*, vol. 220, pp. 524–527, 1983.
[2] A. A. Oraevsky, R. O. Esenaliev, and V. S. Letokhov, "Pulsed laser ablation of biological tissue: Review of the mechanisms," in *Laser Ablation, Mechanisms and Applications*, J. C. Miller and R. F. Haglund Jr., Eds.   New York: Springer-Verlag, 1991, pp. 112–122.
[3] I. Itzkan, D. Albagli, M. L. Dark, L. T. Perelman, C. von Rosenberg, and M. S. Feld, "The thermoelastic basis of short pulsed laser ablation of biological tissue," in *Proc. Nat. Acad. Sci.*, vol. 92, 1995, pp. 960–1964.
[4] R. Srinivasan, "Ablation of polymers and biological tissue by ultraviolet lasers," *Science*, vol. 234, pp. 559–565, 1986.
[5] M. S. Kitai, V. L. Popkov, V. A. Semchishen, and A. A. Kharizov, "The physics of UV laser cornea ablation," *IEEE J. Quantum Electron.*, vol. 27, pp. 302–307, 1991.
[6] J. G. Fujimoto, W. Z. Lin, E. P. Eppen, C. A. Puliafito, and R. F. Steinert, "Time-resolved studies of Nd:YAG laser induced breakdown: Plasma formation, acoustic wave generation, and cavitation," *Invest. Ophthalmol. Vis. Sci.*, vol. 26, pp. 1771–1777, 1985.
[7] D. Stern, R. W. Schoenlein, C. A. Puliafito, E. T. Dobi, R. Biringruber, and J. G. Fujimoto, "Corneal ablation by nanosecond, picosecond, and femtosecond lasers at 532 and 625 nm," *Arch. Ophthalmol.*, vol. 107, pp. 587–592, 1989.
[8] A. Vogel, S. Busch, K. Jungnickel, and R. Birngruber, "Mechanisms of intraocular photodisruption with picosecond and nanosecond laser pulses," *Lasers Surg. Med.*, vol. 15, pp. 32–43, 1994.
[9] P. K. Kennedy, "A first-order model for computation of laser-induced breakdown thresholds in ocular and aqueous media: Part I: Theory," *IEEE J. Quantum Electron.*, vol. 31, pp. 2241–2249, 1995.
[10] X. H. Hu and T. Juhasz, "Study of corneal ablation with picosecond laser pulses at 211 and 263 nm," *Lasers Surg. Med.*, vol. 18, pp. 373–380, 1996.
[11] R. G. Wheeland, "Clinical uses of lasers in dermatology," *Lasers Surg. Med.*, vol. 16, pp. 2–23, 1995.
[12] X. H. Hu, "Efficient use of Q-switched lasers in the treatment of cutaneous lesions," *SPIE Proc.*, vol. 2395, pp. 586–591, 1995.
[13] C. L. M. Ireland, A. Yi, J. M. Aaron, and C. G. Norgan, "Focal-length dependence of air breakdown by a 20-psec laser pulse," *Appl. Phys. Lett.*, vol. 24, pp. 175–177, 1974.
[14] A. E. Siegman, "New developments in laser resonator," *SPIE Proc.*, vol. 1224, pp. 2–14, 1990.
[15] A. E. Siegman, M. W. Sasnett, and T. F. Johnston, "Choice of clip levels for beam width measurements using knife-edge techniques," *IEEE J. Quantum Electron.*, vol. 27, pp. 1098–1104, 1991.
[16] Y. Du, X. H. Hu, M. Cariveau, G. W. Kalmus, and J. Q. Lu, "Optical properties of porcine skin dermis between 900 nm and 1500 nm," *Phys. in Medicine and Biol.*, vol. 46, pp. 167–181, 2001.
[17] C. A. Sacchi, "Laser induced electric breakdown in water," *J. Opt. Soc. Am. B*, vol. 8, pp. 337–345, 1990.

[18]   (1999). The National Institute of Standards and Technology Atomic Spectra Database. [Online]. Available: http://physics.nist.gov/cgi-bin/AtData/main_asd

[19]   D. J. Finney, *Probit Analysis*, 3rd ed.   Cambridge, U.K.: Cambridge Univ. Press, 1971, ch. 3.

[20]   D. Sliney and M. Wolbarsht, *Safety with Lasers and Other Optical Soruces*.   New York: Plenum, 1980, ch. 7.

[21]   M. J. C. van Gemert, S. L. Jacque, H. J. C. M. Sterenborg, and W. M. Star, "Skin optics," *IEEE Trans. Biomed. Eng.*, vol. 36, pp. 1146–1154, 1989.

[22]   N. Bloembergen, "Laser-induced electric breakdown in solid," *IEEE. J. Quantum Electron.*, vol. 10, pp. 375–386, 1974.

[23]   A. Lembares, X. H. Hu, and G. W. Kalmus, "Absorption spectra of the cornea in the far ultraviolet region," *Investigat. Ophthalmol. and Vis. Sci.*, vol. 38, pp. 1283–1287, 1997.

[24]   B. K. Ridley, "Lucky-drift mechanism for impact ionization in semiconductors," *J. Phys. C*, vol. 16, pp. 3373–3388, 1983.

[25]   A. A. Abrikosov, *Fundamentals of the Theory of Metals*.   Amsterdam, The Netherlands: North-Holland, 1988, ch. 4.

Xin-Hua Hu received the B.S. and M.S. degrees in physics from Nankai University, Tianjin, China, in 1982 and 1985, the M.S. degree in physics from Indiana University at Bloomington in 1986, and the Ph.D. degree in physics from University of California at Irvine in 1991.

In 1995, he joined the Faculty of Physics at East Carolina University, Greenville, NC, and established the Biomedical Laser Laboratory (žhttp://bm-laser.physics.ecu.edu). He is currently directing research in soft tissue ablation by nanosecond laser pulses, laser surgery in animal models, tissue optics and spectroscopy, and Monte Carlo and other large-scale parallel computation of light distribution in turbid systems.

Qiyin Fang received the B.S. degree in physics from Nankai University, Tianjin, China, in 1995, and the M.S. degree in applied physics from East Carolina University, Greenville, NC, in 1998, where he is currently working toward the Ph.D. degree in the Biomedical Laser Laboratory.

His research interests include laser-tissue interaction.

Mickael J. Cariveau received the B.S. degree in Zoology from North Carolina State University, Raleigh, in 1996, and the M.S. degree in biology from East Carolina University, Greenville, NC, in 2000, where he is currently working toward the Ph.D degree in biomedical physics.

His research includes study of near-infrared light propagation in skin dermis and soft tissue ablation.

Mr. Cariveau is a member of the Association of Southeastern Biologists and the North Carolina Academy of Science.

Xiaoning Pan received the B.S. degree in 1987 and the Ph.D. degree in physics in 1995 from Nankai University, Tianjin, China.

He was a post-doctoral Fellow at the Department of Precision Instrument Engineering, Tianjin University, Tianjin, China, from 1995 to 1997, and also at the Department of Physics and Astronomy, Rutgers University, New Brunswick, NJ, from 1997 to 1998. From 1998 to 1999, he was a visiting Assistant Professor in the Biomedical Laser Laboratory, East Carolina University, Greenville, NC. His research interests include laser surface physics, medical lasers, fluorescence spectroscopy, cavity quantum effects, thermal radiation, and ultrashort laser pulses.

Gerhard W. Kalmus received the B.A. degree in German from the University of California at Berkeley in 1967, the M.S. degree in biology from Rutgers University, Camden, NJ, in 1974, and the Ph.D. degree in zoology from Rutgers University, New Brunswick, NJ, in 1977.

He is Professor and Director of Graduate Studies in the Department of Biology, East Carolina University, Greenville, NC. His research interests include mechanisms of neurulation, the effect of alcohol on growth parameters during embryonic development, expression of cell surface molecules during morphogenesis, tissue ablation using nanosecond laser pulses, and optical properties of turbid media, including porcine skin.

Dr. Kalmus has been an active member of the Association of Southeastern Biologists, Sigma Xi, AAAS, the Society for Developmental Biology, the Society for In-Vitro Biology, and other professional societies.